SkiDNet: Skip Image Denoising Network for X-Rays

Sandipan Dutta, Shaurya Chaturvedi, Swaraj Kumar, Dr. MPS Bhatia
Department of Computer Engineering
Netaji Subhas University of Technology
New Delhi, India
sandipand.co@nsit.net.in, shauryac.co@nsit.net.in, swarajk.co@nsit.net.in, bhatia.mps@gmail.com

***Abstract*—Medical imaging has evolved to become an essential tool for screening and diagnosing diseases, but they have certain limitations just like every other technology. X-rays, which is one of the most common radiological examinations, is not immune to imperfections. In this paper, we aim to tackle one such imperfection in X-rays, which is the presence of undesirable noises which causes aberrations in the output projections. This makes diagnosis and analysis difficult since such noises shroud the intricate details that these images contain. Distinctive denoising algorithms have been proposed in the past for a spectrum of vision datasets, but a very few of them are for X-rays. We introduce a new denoising network called SkiDNet, a deep learning approach using an encoder-decoder architecture with skip connections of varying length. The network has been trained on the NIH Chest X-Ray Dataset. With the unique properties injected by different types of connections, SkiDNet is able to surpass the performance of existing models. Furthermore, adopting a different approach to weight initialization and batch normalization makes the network more robust. Denoised X-rays obtained from the network were objectively evaluated using different metrics namely mean squared error, peak signal-to-noise ratio, and the structural similarity index.**

I. Introduction

X-ray imaging is widely used in medical diagnosis enabling one to view the inside of the body for potential fractures, tumors, etc. without having to make incisions. X-rays are produced using photons having wavelengths in the range of 0.01 to 10 nm having high penetration ability. An X-ray image is formed when the area under consideration is exposed under X-rays and resulting attenuation is captured. Throughout the years, different systems have been proposed for enhancing X-ray pictures. But such upgrades likewise prompt enhancement of different noises in the produced pictures. Noises such as Gaussian, Poisson, and Salt and Pepper (SAP) are regularly encountered in X-ray images. Promising works have been done in denoising of medical images but denoising of X-ray images remains relatively under-explored.

Image denoising is a classical problem in computer vision; various solutions have been proposed but each with its own limitations. Denoising techniques for medical images can be broadly classified into two categories - using different filters and algorithms[1-19] and using machine learning models[20-32]. Research in the field of machine learning models has shown to surpass the performance of filters used for denoising. In particular, the recent developments in the field of deep learning has further enhanced the performance of denoising tasks. Deep learning models are highly modular and reusable since the same model can be trained for removing different noises from the images.

Building on the previous research explained in detail in Section III, we introduce SkiDNet: a novel deep learning architecture for denoising X-rays with skip connections. National Institutes of Health (NIH) Chest X-Ray dataset has been used for training the deep learning model. The three types of noises aforementioned are manually added to the dataset to construct noisy images which are used for training the model. The training is unsupervised and the model learns to remove different types of noises from the input, a noisy image.

SkiDNet uses skip connections in encoder-decoder architecture for denoising X-rays. It uses two skip connections: Short Range Skip Connection and Long Range Skip Connection. These connections are classified depending on the number of convolutional layers encapsulated by them. Usage of both short and long connections enables the network to learn the training objective efficiently and swiftly. The skip connections coupled with encoder-decoder architecture makes the model suitable for the denoising task.

To evaluate the efficacy of SkiDNet, we tested it with the current state of the art deep learning denoising techniques in medical imaging. For objective evaluation, we employ various metrics such as Peak Signal to Noise Ratio (PSNR), Mean Squared Error (MSE) and Structural Similarity Index (SSIM). We also explain our choice of weight initialization and training methodology in Section IV. In addition to this, we discuss the characteristics and learning behavior of the network in Section V. By carefully testing and evaluating SkiDNet, we aim to establish the success of short and long-range connections in denoising models. The unique paradigm of dual connections adopted in SkiDNet has shown a lot of potential for applications in other medical domains and beyond. Fig. 1 depicts the experimental procedure followed by the authors in this paper.

II. Background

Real world images usually contain departures from the ideal image that should have been produced. Such departures are

978-1-7281-2009-6/$31.00 paper N-20277.pdf

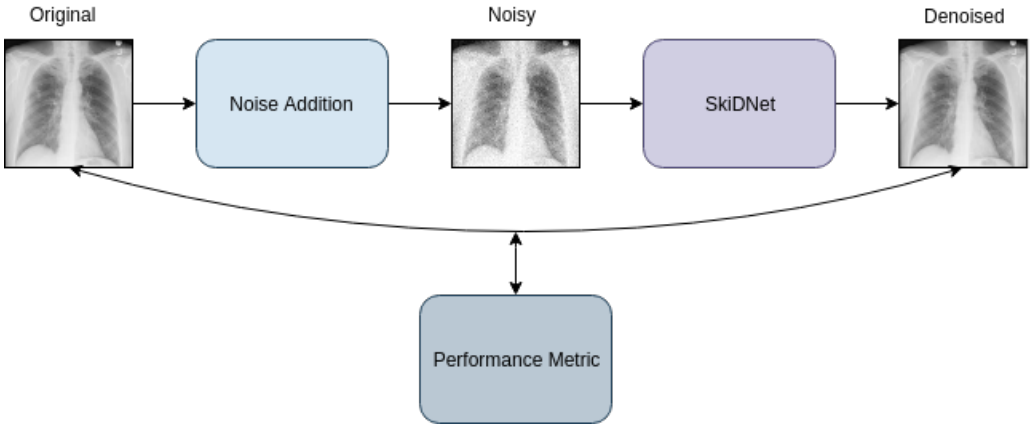

Fig. 1: Figure depicting the proposed experiment. Gaussian, Salt and Pepper and Poisson noises are manually added to the original X-ray images obtained from the dataset. The model is then trained on the prepared dataset and the output images, after denoising, are evaluated using suitable metrics as mentioned in Section V.

referred to as noise. X-ray imaging systems use radiation to capture images. X-ray photons pass through the tissue and interact with the image receptor to produce the image. The underlying principle being followed is the differential absorption of X-ray beams on human body. The image of the bone is produced because more X-rays are absorbed by it than by the surrounding soft tissue. The process of X-ray imaging is plagued by associated noises. Various types of noise often contribute to degrading medical images; some of them have been listed:

A. Gaussian Noise

It is the most common type of noise in independent signals and communication channels. Gaussian noise is a statistical noise having a probability distribution function (PDF) equal to that of the normal distribution:

$$f(x|\mu,\sigma^2) = \frac{1}{\sqrt{2\pi\sigma^2}} e^{-\frac{(x-\mu)^2}{2\sigma^2}} \tag{1}$$

B. Salt and Pepper Noise

Salt and pepper (SAP) noise is also called impulsive noise and is one of the primary noises encountered in X-ray images. This corruption might be caused by a malfunction in X-ray receiver sensors, bit errors in transmission, analog-to-digital converter errors, and faulty memory locations in hardware. SAP noise corrupts pixels, causing the gray levels of the interfered pixels to be either the minimum or maximum values. It can be very easily introduced to an image for an experimental purpose. Given the probability p (with $0 \leq p \leq 1$) that a pixel is corrupted, we can introduce SAP noise in an image by setting a fraction of $p/2$ randomly selected pixels to black (maximum value), and another fraction of $p/2$ randomly selected pixels to white (minimum value).

C. Poisson Noise

Poisson noise is also called quantum or photon noise. X-rays are produced using a photon emitter (quantum) by emitting a certain number of photons per unit time. The quantum noise encountered in X-ray is due to the photons hitting the digital receptor used for producing X-ray. We cannot force them to be evenly distributed over the receptor surface. A particular region of the receptor surface may receive more photons than another region, even when both regions are exposed to the same average X-ray intensity. The noise density in these systems follows the Poisson distribution due to the statistical nature of X-ray photons and thus known as the Poisson noise. A Poisson model assumes that each pixel x of an image $f(x)$ is drawn from a Poisson distribution of parameter $\lambda = f_0(x)$. The Poisson density is given as

$$P(f(x) = k) = \frac{\lambda^k e^{-\lambda}}{k!} \tag{2}$$

III. Related Works

Conventional methods for denoising X-ray images use various filters and algorithms. Elimination of Gaussian Noise has been previously dealt using Gaussian filters[1], anisotropic diffusion[2-4] and bilateral filters[5-6]. In the past, median filters and other nonlinear filters, as well as Wiener filters have been used as restoration methods for images with noise [7]. Another form of noise caused due to corrupted pixels[8], SAP noise has been rectified previously using median filters[9-12]. Weighted Median[13] and weighted mean filters[14] have also been used to remove SAP noise. SAP noise has also been explored in recent works such as the use of pixel-variation gain factors in [8]. [15] uses a new adaptive filtering method by using a multi layered pulse coupled neuron network (PCNN). Other works also explore the reduction of Poisson Noise from X-ray images such as [16] which uses region classification and response median filtering. It has also been rectified using Adaptive Total Variation Regulation[17] and Total Variation Regulation [18]. Raj and Venkateswarlu [19] also discuss Multiscale transforms for denoising of Poisson noise.

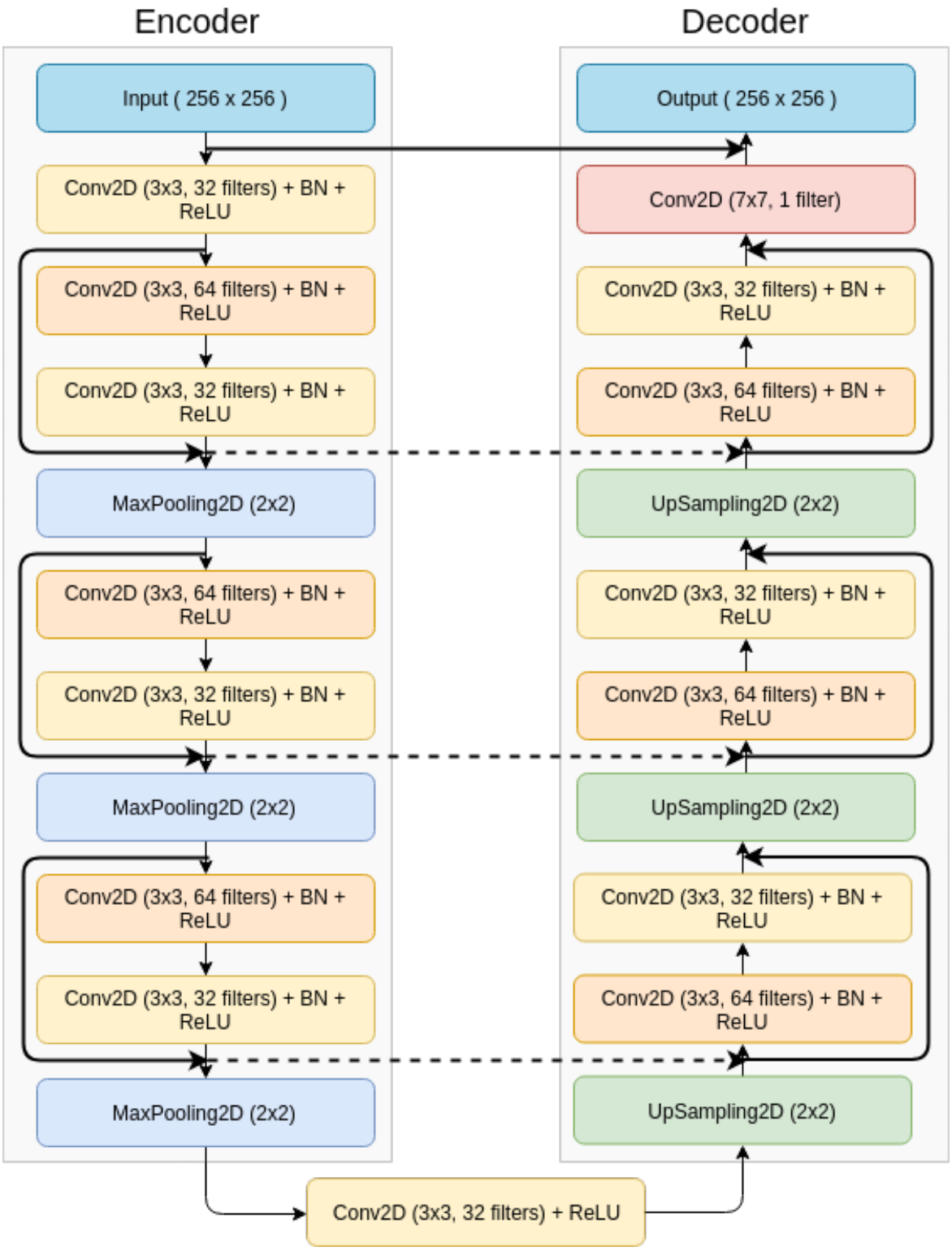

Fig. 2: The architecture of SkiDNet. The convolutional encoder-decoder architecture is combined with short-range and long-range skip connections making the network suitable for the denoising task. The dotted arrows represent a concatenation of the output of particular layers from the encoder to the decoder, whereas the bold arrows represent a residual addition from the preceding layers. Batch Normalization is also used due to its inherent advantages.

Apart from the above-mentioned methods, there has been active research in the application of deep learning for denoising. [20] shows the efficacy of deep learning models for denoising images. In [21], multi-layer perceptron (MLP) was successfully applied for image denoising.

In particular, the performance of convolution neural networks (CNN) was better. Jain and Seung [22] demonstrate the use of CNNs for image denoising. There have been attempts to create denoising models using convolutional encoder-decoder architecture [23] and autoencoders [24]. Stacked Denoising Autoencoder has also been used for removing Gaussian noise from images [25]. Stacked Sparse Denoising Autoencoder (SSDA) [26] gives the best results among denoising autoencoders. Apart from these, DnCNN [27], RED-CNN [28], IRCNN [29] and WGAN-VGG [30] are the most popular denoising CNNs. Neural networks have also been proven to give a much superior performance compared to popular denoising algorithms such as BM3D. [21] have highlighted the strength of using neural networks over BM3D [31]. It highlighted the remarkable ability of the neural network to learn different types of noise, one just needs to provide the training data incorporating that noise. Though some methods mentioned above have been applied to images and not to X-ray images, we incorporate their findings to fine-tune our model. Traditional machine learning models such as k-SVD [32] improve the image quality to a certain degree but suffer from loss of critical structural details.

The efficacy of using skip connections in image denoising task has been verified by [33]. These works have made significant strides in using high-level deep learning architecture in medical imaging.

IV. Our Approach

A. Dataset

For the purpose of this study, the NIH Chest X-ray Dataset [34] is used which comprises of 112,120 frontal-view chest X-ray images of more than 30,000 patients in a 1024*1024 resolution.

B. Data Preprocessing

Since the study required dealing with unsupervised data, labels were discarded while preprocessing the dataset. The dimensions of the X-ray images were reduced to 256*256, effectively reducing the image memory footprint by a factor of 16. Furthermore, pixel values in floating point were bounded into 256 colors, hence further compressing the image by a factor of 8, which enabled 8 times more training images in the same amount of memory. The original clean dataset was then processed by adding the three noises, namely Gaussian, SAP and Poisson noise. For each of the three noises, randomly two-thirds of the original clean images were picked and the chosen noise was added. In this way, each noise was present equally among the dataset. After this preprocessing step, the dataset had 224,240 noisy images. This was divided into training dataset of size 134,544, validation dataset of size 44,848 and test dataset of size 44,848 for training and testing of SkiDNet.

C. Architecture

Denoising of images using neural networks has been vastly explored [20]. We propose a novel encoder-decoder architecture, SkiDNet for the task of denoising X-rays. The proposed model has a convolutional encoder and decoder with new skip connections introduced in it as shown in Fig. 2.

SkiDNet is different from the previous deep learning models due to the presence of two unique connections:

1) **Short range skip connections**
   This connection is inspired by the works of ResNet[35] and was originally proposed by [36-38]. These connections significantly enhance the training of a deep neural network by tackling the vanishing gradient problem and help the model to converge swiftly. They also tackle the degradation problem encountered in deep networks [35].
2) **Long range skip connections**
   These are inspired by the connections in U-Net [39,40]. This type of connection is present between an encoding layer (contracting path) and a decoding layer (expanding path). High-resolution features from the contracting path are combined with the layers in the expanding path. This way we enable low-level spatial feature preservation for better intra-slice context exploration[39]. We also maintain the symmetry between the encoder and decoder.

1) Encoder: The encoder part of the network is responsible for reducing the spatial dimensions of the X-ray image by 16 times, which in theory captures the essential features present in the image while rejecting the noise. The encoder consists of five convolutional layers having a kernel size of $3 * 3$ with the number of filters alternating between 32 and 64. The short range skip connections are made after every two convolutional layers, whereas the long-range skip connections originate from the encoder to the decoder after every alternate convolutional layer. Maxpooling of dimensions $2 * 2$ after every two consecutive convolutional layers reduces the spatial dimensions of the image. The encoder employs batch normalization for normalizing the covariance shift. Rectified Liner Unit(ReLU) as an activation function is added to break the linearity dependence on input.

2) Decoder: The output of the encoder network is a compressed feature representation of the original X-ray image. This is then fed to the decoder in order to reconstruct the denoised image from the feature representations. The decoder network contains five convolutional layers having a kernel size of $3 * 3$ and the number of filters alternating between 32 and 64. This allows the decoder to maintain its symmetry with the encoder. UpSampling layers are added after every alternate convolutional layer in order to increase the spatial dimensions of the image, and short-range skip connections are also added. Long range skip connections originating from the encoder meet the decoder, hence enhancing the restructuring of the denoised image. It is of prime importance to use symmetric layers and connections in encoder and decoder. The advantages of using symmetric network having skip connections in image denoising are well established [33]. While [33] did not explore

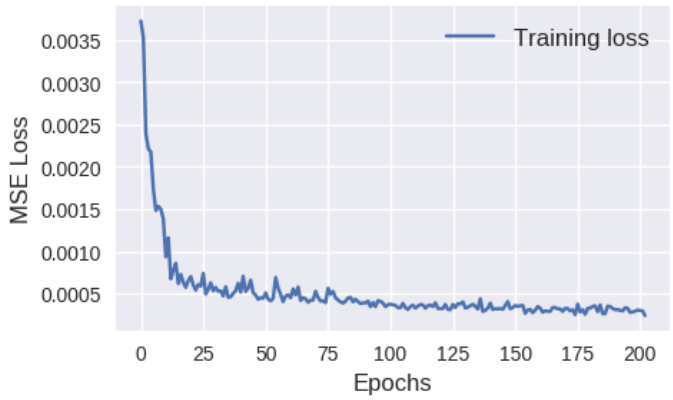

Fig. 3: Training curve depicting the mean squared error loss versus epochs for which the SkiDNet was trained.

the usage of short-range skip connections, the core idea of maintaining symmetry has also been found to be valid in SkiDNet. The decoder network has a final convolution layer of a single channel and kernel size $7*7$ to output the denoised image having the dimensions $256*256$ having a single color channel.

D. Activation Function

To improve the performance of the neural network for speech, we use Rectified Linear Unit (ReLU) as the activation function because it enables sparsity in hidden layer representation. ReLU also offers to disperse values of hidden unit activation probabilities thus ensuring that the information is distributed uniformly in the hidden layer. Dispersion measures whether the set of active units is different for each stimulus [41]. It also enables the network to become invariant to input perturbations [42].

E. Weight Initialization

We initialize the convolutional layers in the network with [43]. The convolution neural networks which are initialized randomly generally have difficulties in converging. As SkiDNet uses ReLU as activation function, weight initialization according to the scheme prescribed by [43] is used. This method provides better initialization by taking ReLU into account.

F. Batch Normalization

Batch Normalization has been used to increase the efficiency of the training process. Neural networks suffer from changes in the distributions of layers inputs during training. This presents a problem because the layers need to continuously adapt to the new distribution, which is known as internal covariate shift. Batch normalization alleviates the internal covariate shift by incorporating a normalization step and a scale and shift step before the non-linearity in each layer[44]. It ensures fast training and better performance of the architecture proposed.

V. Evaluation

The network is trained using Mean Squared Error loss function for 500 epochs. ADAM[45] optimizer is used to minimize the loss. Learning rate of 0.0001 is used for training SkiDNet. Fig. 3 shows the variation of the MSE loss over the number of epochs for which the model is trained.

Comparing the restoration results require a measure of image quality. For objective evaluation of our network, we use the following metrics :

1) MSE: Mean squared error is used for quantitative assessment of the image quality obtained from the SkiDNet. It is one of the most common metrics used for evaluation of the images and is given by:

$$MSE = \frac{1}{M*N}\sum_{1}^{M}\sum_{1}^{N}(F(i,j) - A(i,j))^2 \tag{3}$$

The lower the value of the MSE score, the better the quality of the image obtained as it measures the closeness of denoised image with the original image on a pixel-by-pixel basis.

2) PSNR: It is the ratio between the maximum possible value (power) of a signal and the power of distorting noise that affects the quality of its representation.

$$PSNR = 10\,log_{10}\frac{M*N*255*255}{\sum_1^M\sum_1^N(F(i,j) - A(i,j))^2} \tag{4}$$

A higher PSNR shows that the model has reconstructed the degraded image better to match the original image. As PNSR is inversely related to MSE, we aim to reduce MSE to get a higher PSNR.

3) Structured Similarity Index: Structured Similarity Index or SSIM is also used to compare the images obtained after denoising with the original X-ray images. Unlike PSNR, SSIM is based on visible structures in the image and is used extensively due to its higher accuracy and consistency[46]. SSIM does not strictly rely on numerical comparison but also takes into account the biological factors of the human vision system. It is a composite index of three measures namely image luminance, contrast, and structural changes. Considering x as the original image and y as the output obtained from the denoising model, SSIM is given by

$$SSIM(x,y) = [l(x,y)]^{\alpha}[c(x,y)]^{\beta}[s(x,y)]^{\gamma} \tag{5}$$

where α, β and $\gamma > 0$ control the relative significance of each of three terms in SSIM and l, c and s are luminance, contrast and structural components calculated as

$$l(x,y) = \frac{2\mu_x\mu_y + C_1}{\mu_x^2 + \mu_y^2 + C_1} \tag{6}$$

$$c(x,y) = \frac{2\sigma_x\sigma_y + C_2}{\sigma_x^2 + \sigma_y^2 + C_2} \tag{7}$$

$$s(x,y) = \frac{2\sigma_{xy} + C_3}{\sigma_x\sigma_y + C_3} \tag{8}$$

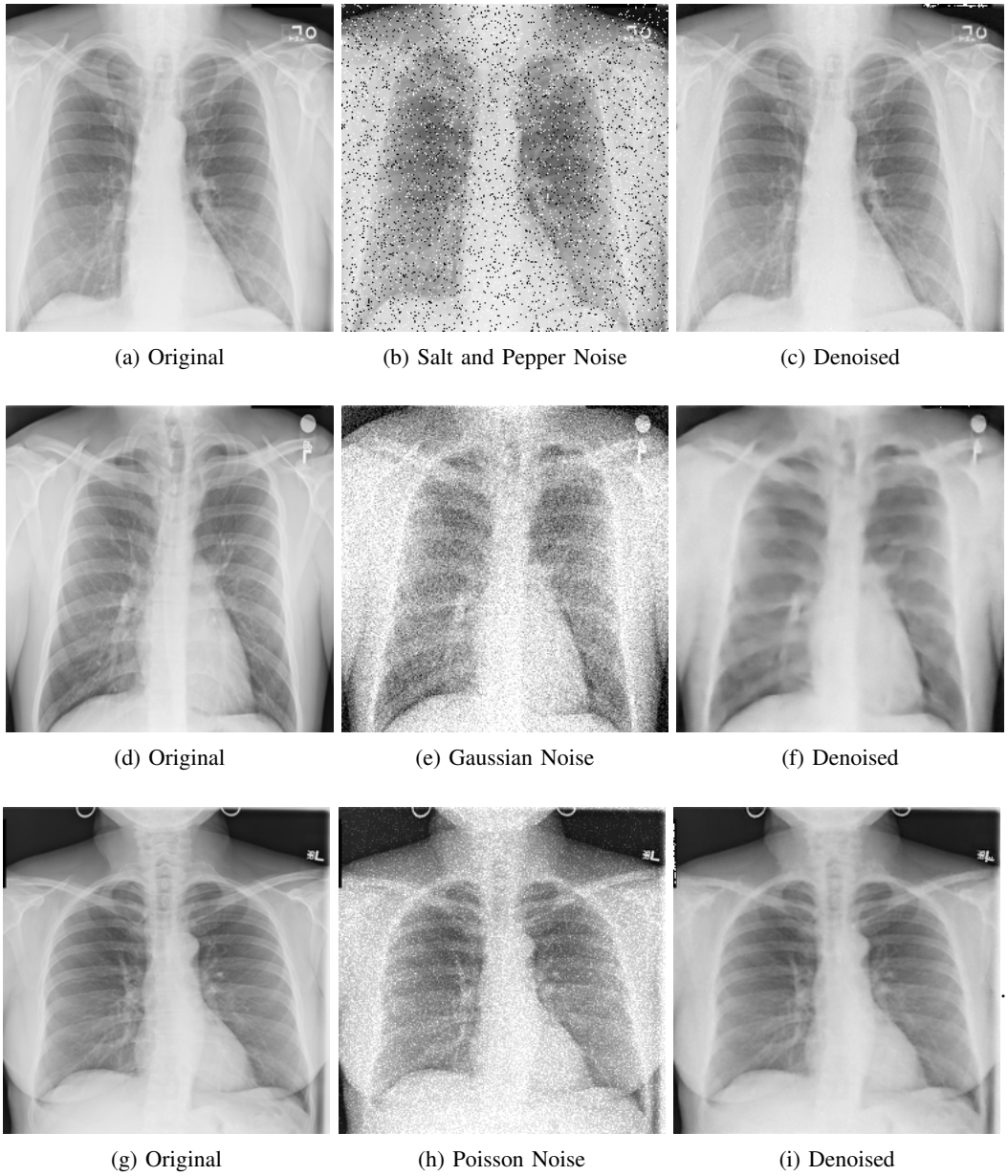

(a) Original (b) Salt and Pepper Noise (c) Denoised

(d) Original (e) Gaussian Noise (f) Denoised

(g) Original (h) Poisson Noise (i) Denoised

Fig. 4: Results obtained after denoising distorted X-rays using SkiDNet, of sample X-ray images containing the three scrutinized noises, i.e. Gaussian, SAP and Poisson. It can be observed from the outputs that the network is able to remove noise from the images irrespective of the type of noise present in the X-ray, thus validating the use of SkiDNet for the task of denoising X-ray images.

where μ_x and μ_y represents the mean of original and denoised image, σ_x and σ_y are standard deviations and σ_{xy} is the covariance of two images[46]. The mean of SSIM scores obtained from the test data is reported for comparison with the existing state of art.

We compare the performance of our network with the existing state of the art networks. Images obtained from SkiDNet are compared with RED-CNN [28], WGAN-VGG [30] and CPCE-2D [23] and SSDA [26]. The results obtained from the different metrics reveal that SkiDNet outperforms all the other networks used for denoising X-ray images. Table

TABLE I: Performance evaluation of SkiDNet against the existing state of the art deep learning models. Popular evaluation metrics such as MSE, PSNR and SSIM are used for comparison.

Models	**PSNR**	**SSIM**	**MSE**(10^{-4})
RED-CNN	37.439	0.922	1.634
WGAN-VGG	33.536	0.875	1.976
CPCE-2D	34.408	0.898	1.664
SSDA	36.952	0.913	1.971
SkiDNet	**38.649**	**0.947**	**1.593**

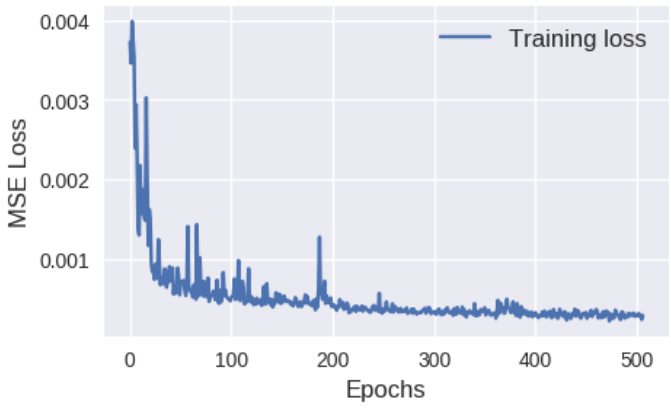

Fig. 5: Training curve depicting the mean squared error loss versus epochs in which the SkiDNet without short range skip connections was trained.

1 highlights this fact where SkiDNet gets a higher score when evaluated using PSNR, SSIM, and MSE. Furthermore, Fig. 4 shows three samples where the SkiDNet removes SAP, Gaussian and Poisson noise from X-ray images thus showing its effectiveness in tackling various noises that may exist in a given image.

The better performance of SkiDNet can be associated with the use of short-range and long-range skip connections together in the network as explained in Section IV. These added connections help denoise the input images better. Moreover, the use of batch normalization helps the model overcome the covariate shift problem making the training more efficient. Table 2 highlights the same fact. These unique additions to SkiDNet make it perform better than the models previously proposed for the task.

Fig. 4 provides an empirical proof of the efficacy of short connections. There is a considerable difference between the training curves in Fig. 3 (SkiDNet with short connections) and Fig. 5 (SkiDNet without short connections). The network neither follows a consistent learning curve in absence of short range skip connections, nor does it converge. These results help us conclude that shortcut connections act as a catalyst for swift convergence, which aligns with the findings of [35] and [47].

Clinical viability of the obtained images was verified by a team of seven medical experts. These included four cardiologists and three radiologists. Each of them was given a set of 200 different denoised X-rays obtained from SkiDNet. Each X-ray was of a person diagnosed with medical complications. The experts had to correctly identify the complications by analyzing the scans. Of the cumulative 1400 denoised images, the doctors were able to correctly diagnose in 1381 images, giving an correct diagnostic accuracy of 98.64%. This further reinforces the efficacy of SkiDNet in removing noises from the X-ray images and maintaining the structural information intact in the X-ray images.

TABLE II: A comparison of the different techniques that have been used in various networks for the denoising of X-rays.

Model	Skip Connections		BatchNorm	Convolutions
	Short	Long		
WGAN-VGG	No	No	No	Yes
RED-CNN	Yes	No	No	Yes
CPCE-2D	No	Yes	No	Yes
SSDA	No	No	No	Yes
SkiDNet	**Yes**	**Yes**	**Yes**	**Yes**

VI. Conclusion

In this paper, we propose a novel denoising technique in the form of SkiDNet. SkiDNet uses an encoder-decoder architecture in addition with skip connections of variable length. The unique skip connections enables SkiDNet to learn the denoising task efficiently and reduce training time for the model. We also demonstrate the ability of SkiDNet to adapt to different noises namely Gaussian, Salt and Pepper and Poisson noise. Performance of SkiDNet exceeds the current state of the art denoising deep learning models in the medical domain, which is verified using multiple objective evaluations. The success of SkiDNet can also be attributed to our approach to weight initialization, batch normalization, and careful hyperparameter tuning. Though we tested our network exclusively on X-rays, the performance of the SkiDNet is an illustration of the new possibilities it offers in medical imaging. Furthermore, our work can be extended to other domains of medical imaging such as CT scans, MRI etc. Simultaneous usage of long and short range skip connections is able to provide precision and accuracy, two characteristics which are essential to medical imaging. Our idea of using skip connections of variable length can be used in other tasks in medical imaging such as segmentation and classification. The application of SkiDNet for mainstream deep learning tasks can offer promising possibilities for new experimentation and innovation.

References

[1] K. Ito, "Gaussian filter for nonlinear filtering problems", In Decision and Control, 2000. Proceedings of the 39th IEEE Conference on (Vol. 2, pp. 1218-1223), IEEE, 2000.

[2] B. Kurt, V.V. Nabiyev, and K. Turhan, "Medical images enhancement by using anisotropic filter and clahe," Innovations in Intelligent Systems and Applications (INISTA), 2012 International Symposium On. IEEE, 2012.

[3] P. Perona, and J. Malik, "Scale-space and edge detection using anisotropic diffusion." IEEE Transactions on pattern analysis and machine intelligence 12.7, 1990: 629-639.

[4] Y. Yu, and S.T. Acton, "Speckle reducing anisotropic diffusion," IEEE Transactions on image processing 11.11 , 2002 : 1260-1270.

[5] S. Paris, P. Kornprobst, J. Tumblin, and F. Durand, "A gentle introduction to bilateral filtering and its applications", In ACM SIGGRAPH 2007 courses (p. 1), ACM, August, 2007.

[6] C. Tomasi, and R. Manduchi, "Bilateral filtering for gray and color images", In Computer Vision, 1998, Sixth International Conference on (pp. 839-846), IEE, January, 1998.

[7] L. Wang, J. Lu, Y. Li, T. Yahagi, and T. Okamoto, "Noise removal for medical X-ray images in wavelet domain," IEEJ Transactions on Electronics, Information and Systems, 126, 2006 ,pp: 237-244.

[8] C.T. Lu, M. Y. Chen, J. H. Shen, L. L. Wang, and C. C. Hsu, "Removal of salt-and-pepper noise for X-ray bio-images using pixel-variation gain factors," Computers and Electrical Engineering,2017.

[9] H. M. Lin, and A. N. Willson, "Median filters with adaptive length," IEEE Transactions on Circuits and Systems, 35(6), ,1988, pp:675-690.

[10] S-J. Ko, and Y. H. Lee, "Center weighted median filters and their applications to image enhancement," IEEE transactions on circuits and systems 38.9, 1991,pp: 984-993.

[11] C. Y. Tsai, "An adaptive rank-ordered median image filter for removing salt-and-pepper noise," Diss. Masters thesis, National Cheng-Kung University, 2006.

[12] H. Hwang, and R. A. Haddad, "Adaptive median filters: new algorithms and results," IEEE Transactions on image processing 4.4, 1995, pp: 499-502.

[13] C.T. Lu,, and T.C. Chou, "Denoising of salt-and-pepper noise corrupted image using modified directional-weighted-median filter," Pattern Recognition Letters 33.10 ,2012,pp: 1287-1295.

[14] Y. Wang, J. Wang,X. Song, and L. Han,"An efficient adaptive fuzzy switching weighted mean filter for salt-and-pepper noise removal," IEEE Signal Processing Letters, 23(11),2016,pp:1582-1586.

[15] X. Deng, Y. Ma, and M. Dong, "A new adaptive filtering method for removing salt and pepper noise based on multilayered PCNN." Pattern Recognition Letters 79, 2016,pp: 8-17.

[16] T. Kirti, K. Jitendra, and S. Ashok, "Poisson noise reduction from X-ray images by region classification and response median filtering," Sdhan 42.6 ,2017,pp: 855-863.

[17] V. B. Prasath, "Quantum Noise Removal in X-Ray Images with Adaptive Total Variation Regularization", Informatica, 28(3), 2017, pp:505-515.

[18] L. I. Rudin, S. Osher, and E. Fatemi, "Nonlinear total variation based noise removal algorithms," Physica D: nonlinear phenomena 60.1-4 ,1992,pp: 259-268.

[19] V. Raj, N. Prudhvi, and T. Venkateswarlu, "Denoising of Poisson and Rician Noise from Medical Images using Variance Stabilization and Multiscale Transforms," International Journal of Computer Applications 57.21 ,2012.

[20] C. Tian, Y. Xu, L. Fei, & K. Yan, "Deep Learning for Image Denoising: A Survey", arXiv preprint arXiv:1810.05052, 2018.

[21] H. C. Burger, C.J. Schuler, and S.Harmeling, "Image denoising: Can plain neural networks compete with BM3D?," Computer Vision and Pattern Recognition (CVPR), 2012 IEEE Conference on, IEEE, 2012.

[22] V. Jain, and S. Seung, "Natural image denoising with convolutional networks," Advances in Neural Information Processing Systems, 2009.

[23] H. Shan, Y. Zhang, Q. Yang, U. Kruger, M. K. Kalra, L. Sun, W. Cong, and G. Wang, "3-D convolutional encoder-decoder network for low-dose CT via transfer learning from a 2-D trained network," IEEE transactions on medical imaging 37, no. 6 ,2018,pp: 1522-1534.

[24] L. Gondara, "Medical image denoising using convolutional denoising autoencoders," Data Mining Workshops (ICDMW), 2016 IEEE 16th International Conference on, IEEE, 2016.

[25] J. Xie, L. Xu, & E. Chen,"Image denoising and inpainting with deep neural networks," In Advances in neural information processing systems,2012, pp. 341-349.

[26] Y. Liu, & Y. Zhang, "Low-dose CT restoration via stacked sparse denoising autoencoders," Neurocomputing, 284, 2018, pp.80-89.

[27] K. Zhang, W. Zuo, Y. Chen, D. Meng, & L. Zhang, "Beyond a gaussian denoiser: Residual learning of deep cnn for image denoising," IEEE Transactions on Image Processing, 26(7),2017, pp:3142-3155.

[28] H. Chen, Y. Zhang, M. K. Kalra, F. Lin , Y. Chen, P. Liao, and G. Wang , "Low-dose CT with a residual encoder-decoder convolutional neural network", IEEE transactions on medical imaging, 36(12),2017, pp:2524-2535.

[29] K. Zhang, W. Zuo, and L. Zhang ,"Learning a single convolutional super-resolution network for multiple degradations" IEEE Conference on Computer Vision and Pattern Recognition, Vol. 6, 2018.

[30] Q. Yang, P. Yan, Y. Zhang, H. Yu, Y. Shi, X. Mou, M. K. Kalra, Y. Zhang, L. Sun, and G. Wang, "Low dose CT image denoising using a generative adversarial network with Wasserstein distance and perceptual loss," IEEE transactions on medical imaging, 2018.

[31] K. Dabov, A. Foi, V. Katkovnik, and K. Egiazarian, "Image denoising by sparse 3-D transform-domain collaborative filtering," IEEE Transactions on image processing 16, no. 8 ,2007,pp: 2080-2095.

[32] M. Aharon , M. Elad, and A. Bruckstein, "K-SVD: An algorithm for designing overcomplete dictionaries for sparse representation," IEEE Transactions on signal processing 54.11, 2006.pp: 4311.

[33] X. Mao, C. Shen, and Y.B. Yang, "Image restoration using very deep convolutional encoder-decoder networks with symmetric skip connections," Advances in neural information processing systems, 2016.

[34] X. Wang, Y. Peng, L. Lu, Z. Lu, M. Bagheri, and R.M. Summers, "Chestx-ray8: Hospital-scale chest x-ray database and benchmarks on weakly-supervised classification and localization of common thorax diseases," In 2017 IEEE Conference on Computer Vision and Pattern Recognition (CVPR), pp. 3462-3471, IEEE, 2017.

[35] K. He, X. Zhang, S. Ren, and J. Sun, "Deep residual learning for image recognition," In Proceedings of the IEEE conference on computer vision and pattern recognition, pp. 770-778, 2016.

[36] C. M. Bishop, ,"Neural networks for pattern recognition," Oxford university press,1995 .

[37] B. D. Ripley, "Pattern recognition and neural networks" ,Cambridge university press ,2007.

[38] W. N. Venables, and B. D. Ripley,"Tree-based methods," Modern applied statistics with S-Plus, Springer, New York, NY, 1999,pp: 303-327.

[39] O. Ronneberger, P. Fischer, and T. Brox, "U-net: Convolutional networks for biomedical image segmentation," International Conference on Medical image computing and computer-assisted intervention, Springer, Cham, 2015.

[40] X. Li, H. Chen, X. Qi, Q. Dou, C. W. Fu, & P. A. Heng, "H-DenseUNet: Hybrid densely connected UNet for liver and liver tumor segmentation from CT volumes," arXiv preprint arXiv:1709.07330, 2017.

[41] B. Willmore, and D.J. Tolhurst, "Characterizing the sparseness of neural codes," Network: Computation in Neural Systems 12.3, 2001, pp: 255-270.

[42] A.La. Maas, A.Y. Hannun, and A.Y. Ng. "Rectifier nonlinearities improve neural network acoustic models." In Proc. icml, vol. 30, no. 1, p. 3, 2013.

[43] K. He, X. Zhang, S. Ren, and J. Sun, "Delving deep into rectifiers: Surpassing human-level performance on imagenet classification." In Proceedings of the IEEE international conference on computer vision, 2015, pp. 1026-1034.

[44] S. Ioffe, and C. Szegedy, "Batch normalization: Accelerating deep network training by reducing internal covariate shift," arXiv preprint arXiv:1502.03167 ,2015.

[45] D.P. Kingma and J. Ba, "Adam: A method for stochastic optimization." arXiv preprint arXiv:1412.6980, 2014.

[46] Z. Wang, A.C. Bovik, H.R. Sheikh, and E.P. Simoncelli, "Image quality assessment: from error visibility to structural similarity," IEEE transactions on image processing 13, no. 4 ,2004, pp: 600-612.

[47] S. Zagoruyko, and N. Komodakis, "Wide residual networks" arXiv preprint arXiv:1605.07146, 2016.